



## Mechanical characterization of basalt fibre reinforced plastic with different fabric reinforcements – Tensile tests and FE-calculations with representative volume elements (RVEs)

Piergiorgio Valentino, Franco Furgiuele

*University of Calabria, Department of Mechanical, Energy and Management Engineering, Ponte P. Bucci, 44C, 87036 Rende (CS), Italy*

Marco Romano, Ingo Ehrlich

*University of Applied Sciences Regensburg, Department of Mechanical Engineering, Laboratory for Composite Technology, Galgenbergstrasse 30, 93053 Regensburg, Germany*

Norbert Gebbeken

*University of the Bundeswehr Munich, Institute for Engineering Mechanics and Structural Mechanics, Werner-Heisenberg-Weg 39, 85577 Neubiberg, Germany*

---

**ABSTRACT.** This paper describes the results of tensile tests and finite element (FE) calculations with representative volume elements (RVEs) of basalt fibre reinforced plastic with two different types of fabric reinforcements. As fabric reinforcements show repeating undulations of warp and fill yarn, simple mixture laws reach their limits. That is the reason why the mesoscopic dimension, lying between the microscopic and the macroscopic dimension, has to be taken into account when a mechanical characterization of fabric reinforced composites is carried out. The aim of this work is to determine the stiffness of a fabric reinforced composite in warp and fill direction with numerical investigations. The simulations are based on FE-calculation with two different RVEs. The tensile tests and the FE-calculations have been carried out for two different types of basalt fabrics, namely twill 2/2 and twill 1/3. The comparison between the experimental data and the results of the FE-calculations are provided in order to support the validity of the proposed model.

**SOMMARIO.** L'articolo descrive i risultati delle prove di trazione e delle simulazioni agli elementi finiti effettuate su compositi a matrice plastica rinforzati con differenti tipologie di tessuti in fibre di basalto. Poiché i tessuti rinforzanti sono caratterizzati da ondulazioni ripetute di trama e ordito la semplice legge delle misture presenta dei limiti. Per questo motivo la scala mesoscopica, via di mezzo tra quella microscopica e macroscopica, è utilizzata per la caratterizzazione meccanica di questa tipologia di compositi.

Lo scopo di questo lavoro è di determinare la rigidità sia nella direzione della trama che in quella dell'ordito dei compositi rinforzati con tessuti. Le simulazioni sono basate sul calcolo agli elementi finiti su due differenti volumi rappresentativi (RVEs). Le prove di trazione e i calcoli agli elementi finiti sono stati effettuati per due diverse tipologie di tessuti in fibre di basalto ossia tessitura 2/2 e tessitura 1/3. Il confronto tra i dati sperimentali e i risultati ottenuti dall'analisi FEM è stato effettuato al fine di validare il modello proposto.

**KEYWORDS.** Basalt fibre; Basalt fibre reinforced plastic; Fabric reinforcement; Woven fabric; Tensile testing; Representative volume element (RVE).

## INTRODUCTION

Simplified theoretical approaches for fibre reinforced plastics often presume a layup of only unidirectional reinforced layers and homogenization approaches for the prediction of structural properties. However, different kinds of fabrics are often applied as reinforcements in the layup of structural parts. A fabric is a two dimensional textile semi-finished product. Warp and fill yarn cross each other in a given pattern. In the composite material the interaction between fibres and matrix are responsible for bearing mechanical loads. The aim of this work is to determine the stiffness of a fabric reinforced composite in warp and fill direction experimentally and by means of numerical simulations using commercial finite element software code. As the mesoscopic geometry of fabric reinforcements is distinctively different compared to unidirectional layers the effect of the repeated undulations of the yarns in warp and fill direction is supposed to influence structural mechanical properties.

Continuous basalt fibres in polymeric matrix systems, especially thermosets, offer great perspectives for structural applications as they have similar or slightly better mechanical properties compared to glass fibres. They are produced in a single-step pultrusion process in which the fibres are directly extracted from a melt of pure basaltic rocks [3, 23]. A widespread technical application, however, does not exist up to now. Therefore an essential reason is the lack of a sound material characterization on the basis of high quality and reproducible semi-finished products such as prepregs for autoclave processing.

In the experimental investigations the processing was done in hand layup with a matrix system curing at room temperature in a vacuum bag. Therefore two different types of dry fabrics, namely twill weave 2/2 and twill weave 1/3, have been used. The determination of the fibre volume content has been carried out as a criterion to evaluate the achieved quality of the produced basalt fibre reinforced plastics. The thereby obtained results are the essential information to validate micromechanical homogenization theories and to predict the structural mechanical properties of the fibre reinforced structure. Preliminary work with comparable material has for example been published in [7].

The models for the numerical investigations are based on the geometric dimension obtained by optical microscopy of the top view of the dry fabric and side view of a cross-section the cured material, respectively. Based on the determined geometric dimensions two RVEs have been modelled. The tow's cross-sections are assumed to be elliptical and a tow undulation was approximated by a steady sinusoidal function.

The purpose of the carried out investigations is to demonstrate that the approach with the finite element modelling is reliable and delivers accurate predictions of the stiffness in the predominant directions. In a further step the FE-calculations can be adopted to other kind of fabric geometries, and thus deliver solutions for other types of similar problems.

## MATERIALS AND TEST PROCEDURES

In the following the material processing and the experimental equipment is described. The procedures to determine the neat resin's and composite material's density, fibre volume content and porosity voids are briefly mentioned. The respective standards (DIN, EN or ISO) are indicated. In Tab. 1 the structural mechanical properties of both the basalt fibres and the epoxy resin are listed. They have been extracted from the respective data sheet [17, 18]. The values listed for basalt fibres imply the fibres itself as a homogeneous isotropic material.

### *Processing*

Several test panels have been produced by hand layup in vacuum bag processing. The processing was done with an epoxy matrix system curing at room temperature [17] in a vacuum bag. Fig. 1 shows a scheme of the layup used for the test panel fabrication for the specimens. All test panels have been produced using the same matrix system [17] in order to achieve entirely comparable specimens.

The used semi-finished products and the corresponding layups are listed in Tab. 2. Two different types of fabrics have been used. These are namely twill 2/2, twill 1/3 [18]. The notation 2/2 indicates that the every second warp yarn is undulated by the fill yarn, whereas the notation 1/3 indicates that repeatedly three and one warp yarns are undulated by the fill yarn. The following Tab. 2 contains details concerning the technical data of the two kinds of fabrics according to the respective data sheet [18] provided. The aim was to obtain specimens with two thicknesses of approx. 2 mm following DIN EN 2747 [14].



The polymeric matrix system is a cold curing thermoset. The two component epoxy resin is characterized by low viscosity at room temperature, a polymerization temperature starting at 12 °C and a pot life of approx. 40 min [17]. The before mentioned properties characterizes the resin for being quite suitable for hand layup processing.

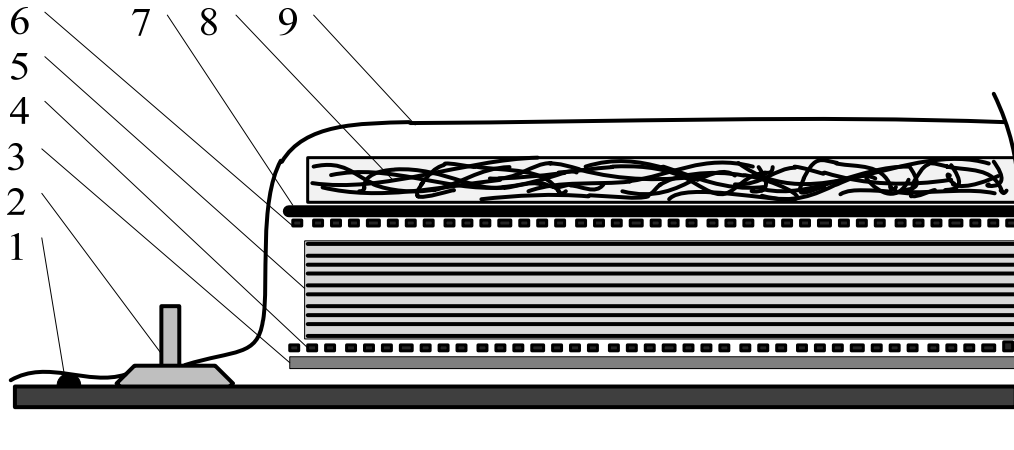


Figure 1: Scheme of the layup used in the processing: 1 sealant tape, 2 vacuum connector, 3 release film, 4 peel ply, 5 composite layup, 6 peel ply, 7 perforated foil, 8 bleeder, 9 vacuum bag.

| Basalt fibres              |                        | Epoxy resin           |                        |
|----------------------------|------------------------|-----------------------|------------------------|
| Mechanical Property        | Value                  | Mechanical Property   | Value                  |
| Density $\rho$             | 2.75 g/cm <sup>3</sup> | Density $\rho$        | 1.15 g/cm <sup>3</sup> |
| YOUNG's modulus $E_1$      | 89 GPa                 | YOUNG's modulus $E$   | 2.65 GPa               |
| YOUNG's modulus $E_2$      | 89 GPa                 | Shear modulus $G$     | 0.98 GPa               |
| Shear modulus $G_{12}$     | 21.7 GPa               | POISSON's ratio $\nu$ | 0.35                   |
| Shear modulus $G_{23}$     | 21.7 GPa               |                       |                        |
| POISSON's ratio $\nu_{12}$ | 0.26                   |                       |                        |
| POISSON's ratio $\nu_{23}$ | 0.26                   |                       |                        |

Table 1: Values of the structural mechanical properties: Left: Basalt fibres [18]. Right: Epoxy resin [17].

### Experimental Equipment

The experimental equipment for preparation, procedure, and evaluation of the tensile test besides common laboratory devices contains, [5, 9]:

- Tensile testing machine INSTRON 8501,
- Hydraulic wedge grips type 647 by MTS SYSTEMS CORPORATION,
- Extensometer,
- Muffle furnace CARBOLITE EML 11/6, which reaches a temperature of 620 °C within a tolerance of 1 °C that is required to evaporate the polymeric matrix completely without effecting the reinforcement [5, 6, 24, 25],
- Precision balance METTLER TOLEDO 204-S being able to supply an accuracy of measurements in a range of 0.1 mg and
- Ceramic containers, which possess a sufficient constancy in mass before and after application of the respective temperature.

The preliminary mentioned experimental equipment fulfil the requirements of the German standards DIN EN ISO 2747 [14] concerning the tensile test and DIN EN ISO 1172 [15] concerning the determination of the fibre volume content by calcination.



| Type of fabric | Type of yarn            | Specific weight in g/m <sup>2</sup> | Warp yarns per cm | Fill yarns per cm | Layup                 | Layers | Thickness in mm | Fibre volume content $\rho_f$ in % |
|----------------|-------------------------|-------------------------------------|-------------------|-------------------|-----------------------|--------|-----------------|------------------------------------|
| Twill 2/2      | Thread of direct roving | 334                                 | 16                | 9                 | [0°/90°] <sub>6</sub> | 6      | ~1.8            | 51.85                              |
| Twill 2/2      | 11.5 μm<br>110 tex      | 334                                 | 16                | 9                 | [90°/0°] <sub>6</sub> | 6      | ~1.8            | 47.88                              |
| Twill 1/3      | Direct roving           | 362                                 | 18                | 8                 | [0°/90°] <sub>6</sub> | 6      | ~1.9            | 49.17                              |
| Twill 1/3      | 11.5 μm<br>110 tex      | 362                                 | 18                | 8                 | [90°/0°] <sub>6</sub> | 6      | ~1.8            | 54.75                              |

Table 2: Types of fabrics, specific weights and layups used.

#### *Determination of fibre volume content*

In [12, 19, 28] basalt fibres are reported to have a very high thermal resistance. Furthermore the diminution of mass of the basaltic fibres due to thermal load is reported to be negligible [5, 24]. Five specimens for each test panel have been weighted before and after the thermal treatment following DIN EN ISO 1172 [15] that is originally intended for glass fibre reinforced plastics.

At five representative positions specimens with dimensions of approx. 20 mm x 10 mm following DIN EN 2559 [13] have been cut off by water jet. The positions are evenly distributed over the respective test panels. The experimentally determined results have been treated in a statistical manner in order to obtain averaged values for each test panel.

The determination of the fibre volume content has been determined by using the above mentioned muffle furnace. The polymeric matrix gets evaporated thermally, i.e. is reduced to ashes, whereas the basalt fibres remain.

By using the before determined density of the neat resin and the density of the basalt fibres out of its technical data sheet [18] and various literature [3, 7, 23] the fibre volume content,  $\phi_f$ , is calculated following DIN EN 2559 [13] from

$$\phi_f = \frac{V_f}{V_c} = \frac{V_f}{V_f + V_m} = \frac{m_f / \rho_f}{\frac{m_f}{\rho_f} + \frac{m_c - m_f}{\rho_m}} \quad (1)$$

where the subscripts *f*, *m* and *c* indicate the fibre, matrix and composite properties, respectively, *V* is the volume, *m* is the mass and  $\rho$  is the density.

The fibre volume content is an indicator for the achieved quality and serves as a base for the prediction of the structural mechanical properties of the single components' properties matrix and fibre reinforcement. The indicated fibre volume contents in Tab. 2 have been determined according to the German standard DIN EN ISO 1172 [15].

The indicated values have been achieved by weighing specimens of approximately approx. 20 mm x 10 mm before and after evaporation of the polymeric matrix system in the previously mentioned muffle furnace. The therefore required densities of the single components have been taken from the data sheet of the matrix system (see Tab. 1) with 1.15 g/cm<sup>3</sup> [17] and the reinforcement fibres with 2.75 g/cm<sup>3</sup> [18], respectively. The achieved values partially seem to be quite elevated regarding the production by hand layup in vacuum bag processing. Values of approximately 40-45 % for the fibre volume content could be expected [26]. In order to exclude that the measured weight of the fibres decreases, the constancy of mass has been validated e. g. in [24, 25], where the constancy of mass under thermal load has been proved experimentally. Thus the experimentally determined values have to be considered plausible.

#### *Geometric dimensions and preparation of specimens for tensile test procedure*

For the experimental determination of the structural mechanical properties specimens have been cut out of the test panels indicated in Tab. 2. The cutting was done according to the German standard DIN EN 2747 [14] by water jet cutting and grinded to the required parallelism of the cutting edge. The obtained tensile test specimens have the plane dimensions of 250 mm x 25 mm with the respective thickness of approximately 2 mm. The application of tabs on both sides and at both ends inhibits the failure of the specimens in vicinity of the clamping. Fig. 2 shows the tabs in the side view of the tensile test specimens.

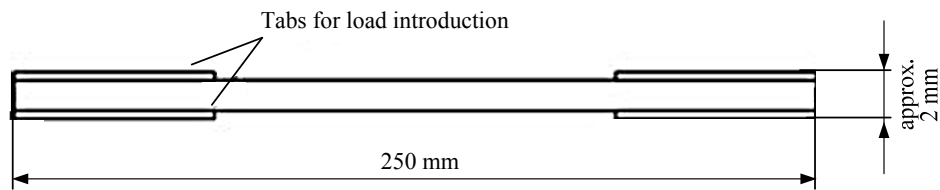


Figure 2: Side view of the tensile test specimens with tabs according to German standard DIN EN 2747 [14].

## INVESTIGATIONS BY FINITE-ELEMENT-ANALYSES

In order to further investigate the influence of the two different types of fabric reinforcement on the structural mechanical properties calculations with the Finite-Element-Analyses have been carried out. The FE-simulation is carried out in a commercial software. Therefore representative volume elements have been modelled by the CAD software and imported into the FE-environment.

### *Determination of geometric dimensions and modelling of the Representative Volume Element (RVE)*

The first step of the FE-analyses requires the geometrical definition and modelling of a representative volume element (RVE) of the considered sample. The classical theory of micromechanics defines a RVE as the smallest sample region, which behaves in the same way as the whole sample.

In order to determine the geometric dimensions of the RVE, top view of the dry fabric and side view of a cross-section of the test panels have been investigated under the optical microscope. The pictures taken provide information about length and width of the respective RVE. Additionally information from the data sheet was used for properly matching the geometric dimensions.

Fig. 3 schematically shows the geometric dimensions of the cross-section of a single lamina in mm. For a proper matching the height of the RVE was additionally obtained by dividing the thickness of each test panel by the number of constituent laminas.

The modelling of the RVE was done very effectively by the commercial software CAD. Based on the determined geometric dimensions the step by step modelling is done as follows:

1. Modelling warp and fill yarn (corresponds to the dry fabric)
2. Separately modelling the surrounding matrix.
3. Finally assembling the fabric and the matrix to the final geometric model of the RVE.

Fig. 4 shows the final RVEs for both types of fabric reinforcements in the CAD-System illustrated as wireframe graphics. For reasons of analytical characterization two simplifying presumptions are necessary. First the geometrical modelling of the direction of warp and fill yarn is carried out by the means of custom-made splines defined within the CAD environment. These are presumed to have a sinusoidal shape, which can be expressed as [11, 20]

$$y = A \cos\left(\frac{2\pi x}{c}\right) \quad (2)$$

where  $A$  is the amplitude of the tow path curve, and  $c$  is the pitch of the tow path curve. The perpendicular cross-sections of warp and fill yarn, respectively, are presumed to have an elliptical shape, where  $a$  and  $b$  are the major and minor semi-axes, respectively [1, 21]. The two simplifying presumptions are illustrated in Fig. 5.

After assembling the fabric and the matrix the final geometric model of the RVE is obtained. Thus the model is ready for further use in the FE-analyses and is imported into FEM software pre-processor-environment.

### *Mesh, contact definitions and assignment of material properties*

For a proper meshing of the three different regions, namely warp yarns, fill yarns and pure matrix, the following definitions in the meshing-environment have been defined. Thereby special attention was put on the orientation of the yarns' reference systems. The yarns are assumed to behave linear elastically and to show orthotropic material properties along the respective predominant directions, which is the fibre direction. As a consequence it is necessary to define the materials' elastic constants continuously following the undulated yarn. Therefore two additional reference systems are introduced, of which one is for assigning the properties to the warp yarns and the other one for assigning the properties

to the fill yarns, respectively. The pure matrix is assumed to be homogeneous and to behave linear-elastically, showing isotropic material behaviour. This assumption requires no further specification of the mesh's orientation.

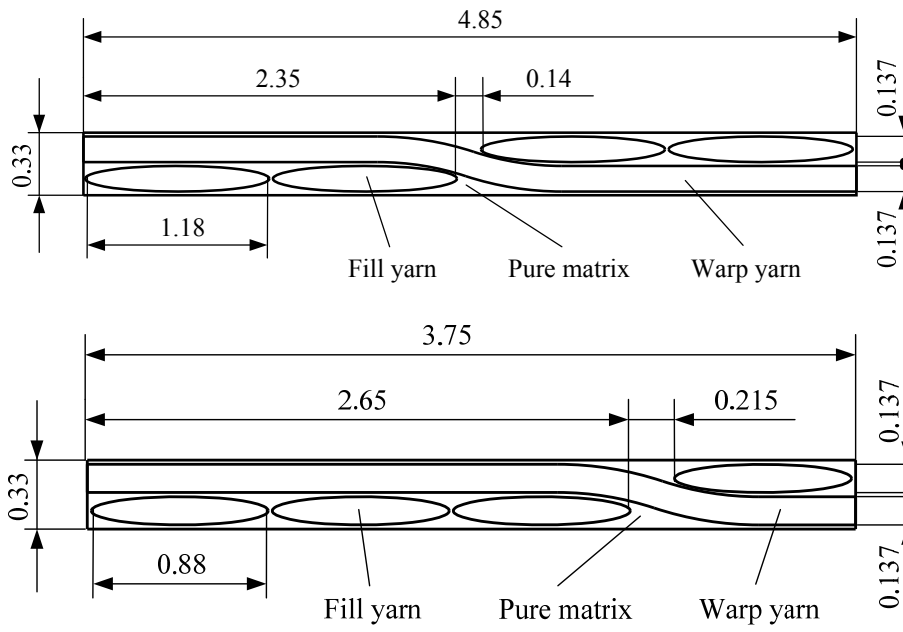


Figure 3: Schematic cross-sections of the two types of dry fabric reinforcements based on pictures taken by an optical microscope that provide the geometrical dimensions in mm of the RVE: Top: Twill wave 2/2. Bottom: Twill wave 1/3.

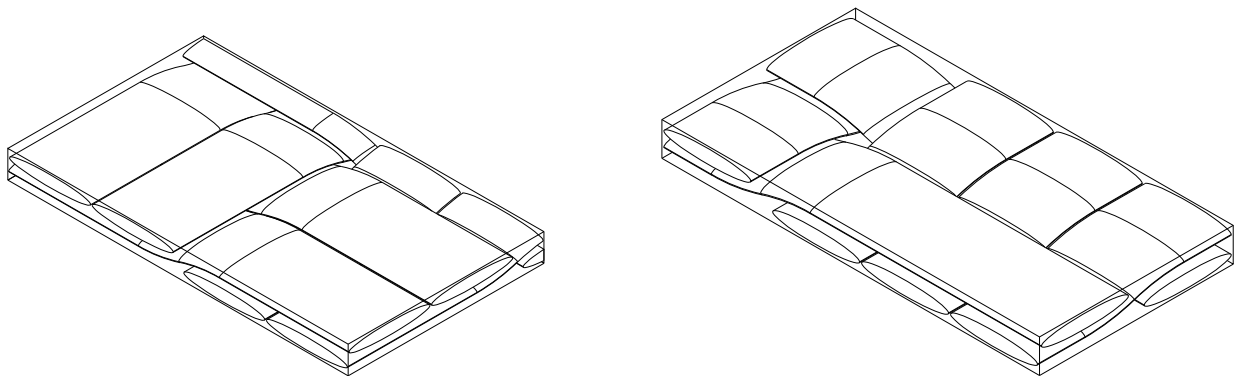


Figure 4: Wireframe graphic of the RVEs in the CAD-System: Left: Twill weave 2/2. Right: Twill weave 1/3.

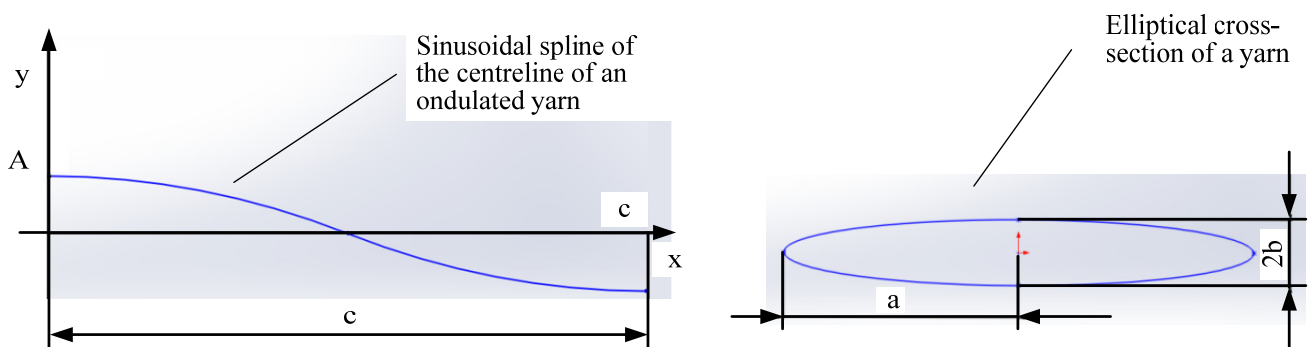


Figure 5: Simplifying presumptions for analytical characterization of the geometry: Left: Sinusoidal spline of the centreline of an undulated yarn. Right: Elliptical cross-section of a yarn.

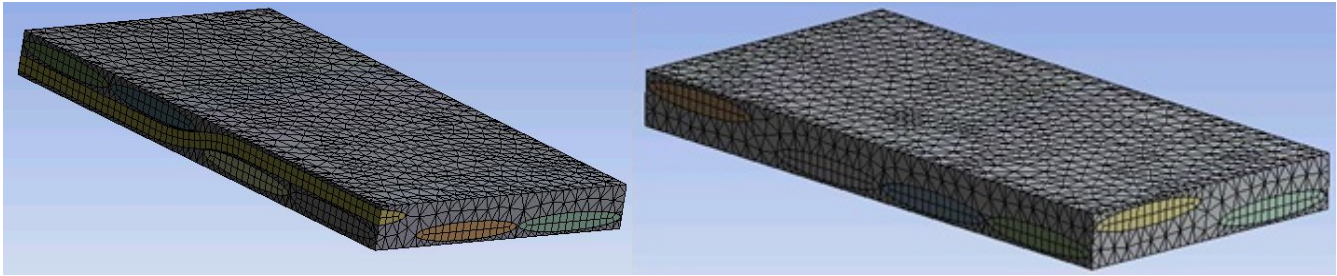


Figure 6: Meshed RVEs in the FE pre-processor : Left: Twill weave 2/2. Right: Twill weave 1/3.

As a first approach an idealized contact is obtained by coincident nodes, where failure mechanisms and friction effects are neglected. The so defined perfect adhesion between fibres and matrix assumes no relative displacement in the contact regions between the three different regions, warp yarns, fill yarns and pure matrix.

The following mesh generation is carried out automatically by the software, considering elements of adequately sufficient size. Fig. 6 shows the meshed RVE for the twill weave 2/2 and twill weave 1/3, respectively.

The matrix surrounding the yarns is presumed to show homogeneous isotropic material behaviour in a completely linear-elastically manner. So the structural mechanical properties of the pure epoxy resin listed in the right part of Tab. 1 are directly assigned to the surrounding matrix.

In contrast the material properties to assign to the yarns have to be calculated as these are the only reinforced regions of the RVEs. The calculation of the material properties is based on the experimentally determined value of the fibre volume content  $\phi_f$ . The experimentally determined value of the fibre volume content is a representative overall value for the specimens cut out of the respective test panel. These values are presumed as the fibre volume content of the whole RVE. Yet the distribution of the fibre volume content and the predominant directions caused by the orientation of the yarns in the RVE is discretely allocated. Only the yarns are fibre reinforced regions whereas the surrounding polymeric matrix system contains no fibre reinforcement at all. Thus the fibre volume content of only the yarns is higher than the experimentally determined value. As an approach the relation of the volumes of the different regions in the RVE is taken as a basis for calculating the fibre volume content by means of a weighted average. Thus the fibre volume content in the yarns of the RVE  $\phi_{f,y}$  can be derived by

$$\phi_{f,y} = \frac{V_{RVE}}{V_y} \phi_{f,c} = \frac{1}{x_y} \phi_{f,c} \quad (3)$$

where the subscripts  $f$ ,  $y$  and  $c$  indicate the fibre, yarns and composite properties, respectively,  $\phi_f$  is the fibre volume content,  $V$  is the volume and  $x$  is relative volume of the yarns in the RVE.

The experimentally determined values for the fibre volume content taken from Tab. 2 are resumed in Tab. 3. The relations of the volumes in the RVEs used for the calculation of the fibre volume content of only the yarns are listed. For verification of the FE-analyses the calculations with the two RVEs are carried out for two calculated fibre volume fractions in the RVEs. The first fibre volume content used for calculating the mechanical properties in the FE-analyses are based on the experimentally determined values  $\phi_f$ . The second ones are based on a standardized value for the fibre volume content  $\phi_f = 50\%$ . The corresponding calculated values for  $\phi_{f,y}$  are listed in Tab. 3.

The afore described procedure for the calculation of the fibre volume contents in the reinforced regions of both RVEs, namely warp and fill yarns, is a linear approach by means of a weighted average. The calculated values of the fibre volume content  $\phi_f$  that are assumed for assigning the structural mechanical properties in the FE-analyses are based on the relative volumes of the different regions in the RVEs and on the experimentally determined values. So the parameters that affect the described approximation are the geometric dimensions of the yarns, the thickness of the RVEs [1], [7], [8] as well as the precision of the experimental determination of  $\phi_f$ .



| Type of fabric and test direction | $\phi_f$ determined experimentally | Region in the RVE   | Relative volume $x$ in the RVE | $\phi_{f,y}$ based on exp. values | $\phi_{f,y}$ standardized to 50 % in the RVE |
|-----------------------------------|------------------------------------|---------------------|--------------------------------|-----------------------------------|--|
| <b>Twill weave 2/2 Warp 0°</b>    | 51.85 %                            | Warp and fill yarns | 76.00%                         | 68.22%                            | 65.79%                                       |
|                                   |                                    | Polymeric matrix    | 24.00%                         |                                   |  |
| <b>Twill weave 2/2 Fill 90°</b>   | 47.88 %                            | Warp and fill yarns | 76.00%                         | 63.00%                            | 65.79%                                       |
|                                   |                                    | Polymeric matrix    | 24.00%                         |                                   |  |
| <b>Twill weave 1/3 Warp 0°</b>    | 49.17 %                            | Warp and fill yarns | 79.00%                         | 62.24%                            | 63.29%                                       |
|                                   |                                    | Polymeric matrix    | 21.00%                         |                                   |  |
| <b>Twill weave 1/3 Fill 90°</b>   | 54.75 %                            | Warp and fill yarns | 79.00%                         | 69.30%                            | 63.29%                                       |
|                                   |                                    | Polymeric matrix    | 21.00%                         |                                   |  |

Table 3: Calculated values to assume for the fibre volume content  $\phi_f$  in assigning structural mechanical material properties in FE-analyses based on the experimentally determined values and the relative volumes of each region in both RVEs.

The yarns are considered as unidirectional reinforced regions. Therefore the material is supposed to behave like a transversally isotropic material with its predominant direction coinciding with the longitudinal direction of the yarn. For assigning this material behaviour to the FE-model the input mask of the orthotropic materials in the FE-pre-processor is used. Nine elastic constants, from which five are independent, are required for assigning the transversally isotropic properties to the reinforced regions of the RVE. Their calculation is described in the following.

The stiffness in the predominant direction is calculated by the weighted average

$$E_1 = \phi_{f,y} E_f + (1 - \phi_{f,y}) E_m \quad (4)$$

As the basalt fibre itself and the polymeric matrix is considered as homogeneous isotropic, the respective shear modulus can be calculated with its respective YOUNG's modulus  $E$  and POISSON's ratio  $\nu$  by  $G = \frac{E}{2(1+\nu)}$ , where the corresponding values are listed in Tab. 1. Rules of mixture according to CHAMIS [2], [10], [26], [27] are applied in order to calculate further three independent linear-elastic properties of the yarns, namely

$$E_2 = E_3 = \frac{E_m}{1 - \sqrt{\phi_{f,y}} \left(1 - \frac{E_m}{E_f}\right)} \quad (5)$$

$$G_{12} = G_{13} = \frac{G_m}{1 - \sqrt{\phi_{f,y}} \left(1 - \frac{G_m}{G_f}\right)} \quad \text{and} \quad (6)$$

$$\nu_{12} = \nu_{13} = \phi_{f,y} \nu_f + (1 - \phi_{f,y}) \nu_m \quad (7)$$

As one of the remaining independent structural mechanic material constants the POISSON's ratio  $\nu_{21}$  is obtained by applying the reciprocal work theorem according to MAXWELL-BETTI,  $E_i \nu_{ji} = E_j \nu_{ij}$ , and so

$$\nu_{21} = \nu_{31} = \frac{E_2}{E_1} \nu_{12} \quad (8)$$

follows. The last remaining independent structural mechanic material constant is the shear modulus  $G_{23}$  that in the carried out investigations is calculated according to CHAMIS [2], [10], [26], [27] by

$$G_{23} = G_{32} = \frac{G_m}{1 - \sqrt{\phi_{f,y}} \left(1 - \frac{G_m}{G_{f,23}}\right)} \quad (9)$$





From equation (9) the POISSON's ratio  $\nu_{23}$  can directly be calculated because it is a dependent structural mechanical property due to the plane of isotropy by  $\nu_{23} = \nu_{32} = \frac{E_2}{2G_{23}} - 1$ .

### Boundary Conditions

In order to apply normal loads on the cross-sections of both RVEs in warp and fill direction, respectively, the boundary conditions are defined as follows.

A clamped cross-section is defined on one cross-section of the RVE. The opposite cross-section is defined as a free cross-section where the loads will be applied as described in the following. The boundary conditions for the nodes on the free cross-section are set in a manner that under the applied load the cross-sections undergo uniform displacements parallel to the applied load. In order to avoid twisting and bending effects due to the asymmetric constructions of both RVEs, symmetric deformation is assured by defining further constraints on the upper and lower surface as well as on the two remaining lateral surfaces. Furthermore on one lateral surface a remote displacement condition is defined in order to suppress the rotational degrees of freedom. The in this manner defined boundary conditions

1. ensure a purely longitudinal deformation,
2. allow contraction of the cross-sections due to POISSON effects over the complete length, width and height and
3. avoid twisting and bending effects.

The afore described boundary conditions assure a properly constrained FE-model for the carried out calculations. As both RVEs are considered in both warp and fill direction, respectively, the boundary conditions have to be adopted for every RVE twice, namely twill weave 2/2 in warp (0°) and fill (90°) direction and twill weave 1/3 in warp (0°) and fill (90°) direction. Thus four independent FE-analyses are carried out as described in the following.

### Application of loads, post-processing and calculation of the respective stiffnesses

The loads are applied on the free cross-section opposite to the clamped one. The respective maximum of the applied load is taken according to the type of fabric and the predominant direction to be investigated. The used maximum loads are the standardized determined tensile strengths illustrated in the following Fig. 7.

As the relevant output dimension of the quasi-static analyses the displacement of the free cross-section in direction of the applied load is extracted from the FE-model. For the determination of the respective stiffnesses the following calculations are carried out for both RVEs in warp and fill direction, respectively. The definition of the normal strain parallel to the applied load

$$\varepsilon = \frac{\Delta l}{l_0} = \frac{l_0 - l_1}{l_0} \quad (10)$$

is calculated, where  $l$  is the geometric dimension of the RVE in direction of the applied load, the subscripts 0 and 1 indicate the state before and after deformation. The stiffness is calculated by

$$E = \frac{\sigma}{\varepsilon} \quad (11)$$

where  $\sigma$  is the applied load,  $\varepsilon$  is the calculated normal strain parallel to the applied load .

## RESULTS AND DISCUSSION

The results of the stiffnesses obtained by the experimental tensile tests and the FE-analyses with both RVEs are confronted graphically and discussed. Additionally the experimentally determined tensile strengths and corresponding failure modes are presented and discussed. The validity, the potentials and limits of the FE-analyses are shown.

### Experimentally and numerically determined stiffnesses

Width and thickness of the specimens have been determined by measuring five times at three representative positions and afterwards averaged. Based on the obtained force-displacement-diagrams and the geometric dimensions the respective stress-strain-diagrams are obtained [9].



Using the weighted average as a first approximation [26], [27], the stiffnesses of the specimens have been calculated as secant modulus  $E_{s,0.5\%}$  at a strain of  $\varepsilon = 0.5\%$  and tangent modulus  $E_{t,0.1\%}$  (as a Secant Modulus at a strain of  $\varepsilon = 0.1\%$ ) according to German standard DIN EN 2747 [14].

For each textile specimens and layup the average values and standard deviations have been calculated, respectively [4], [16], [22]. Fig. 8 and Fig. 9 show the stiffnesses related to each textile semi-finished product as secant modulus  $E_{s,0.5\%}$  and tangent modulus  $E_{t,0.1\%}$  with the respective standard deviations. Whereas Fig. 8 shows the secant moduli and tangent moduli based on the absolute experimentally determined values of the fibre volume content Fig. 9 shows them standardized to a fibre volume content  $\varphi_f = 50\%$ . The results for the YOUNG'S modulus obtained in the FE-simulations carried out for the respective presumed fibre volume contents are displayed as well.

The stiffnesses indicated in Fig. 8 and Fig. 9 as secant moduli  $E_{s,0.5\%}$  and tangent moduli  $E_{t,0.1\%}$  based on the absolute experimentally determined fibre volume content and on the standardized fibre volume content of  $\varphi_f = 50\%$ , respectively, show a distinct difference between the warp and weft direction for the textile reinforced specimens. Tangent moduli  $E_{t,0.1\%}$  slightly exceed the secant moduli  $E_{s,0.5\%}$ . The respective standard deviations are sufficiently small, so that the determined values can be considered as the representative mechanical properties for the textile semi-finished products and their respective dependence on the predominant mechanical properties in warp and weft direction.

The numerically determined stiffnesses show good agreement with the corresponding experimental ones. For both investigated fibre volume contents, namely at first based on the absolute experimentally determined one and second based on the standardized one  $\varphi_f = 50\%$ , the stiffnesses determined by the FE-analyses lies in the range of the secant modulus  $E_{s,0.5\%}$  and the tangent modulus  $E_{t,0.1\%}$ , especially when the respective standard deviations are taken into account. As an exception the numerical results for the stiffness of the twill weave 1/3 in fill direction yield slightly lower values than the experimentally ones.

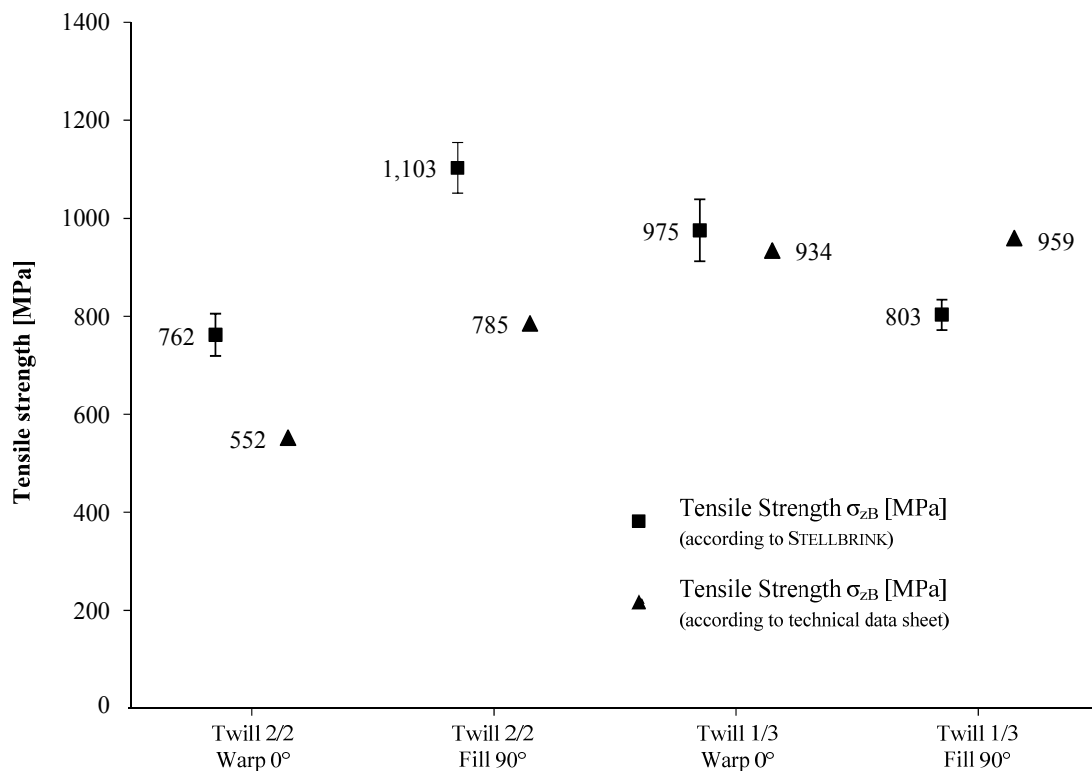


Figure 7: Calculated tensile strengths of the respective textile semi-finished products standardized to a fibre volume content of  $\varphi_f = 50\%$  according to STELLBRINK [27] and data sheets [18].

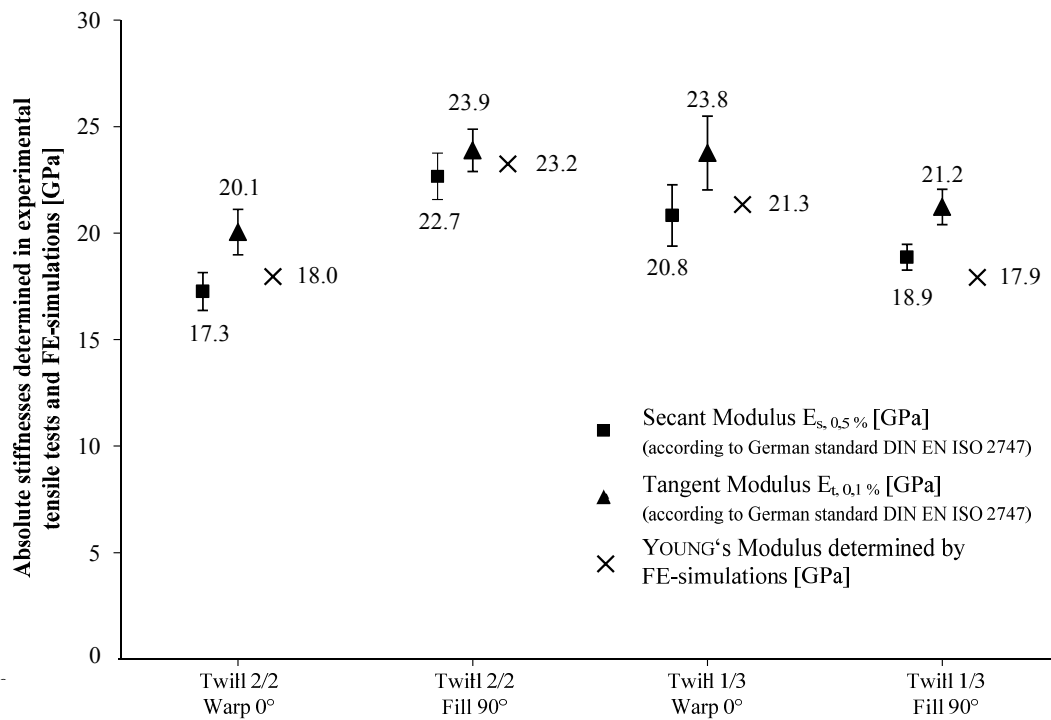


Figure 8: Secant modulus and tangent modulus of the respective textile semi-finished products based on the absolute experimentally determined values of the fibre volume content of  $\varphi_f$  according to German standard DIN EN ISO 2747 [14].

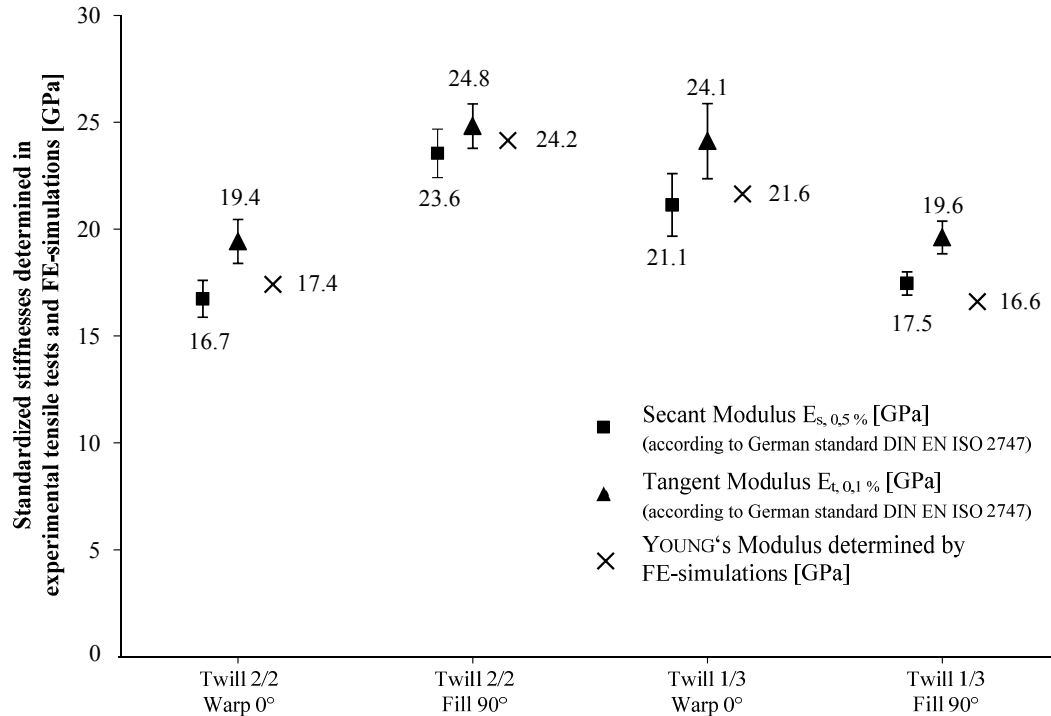


Figure 9: Secant modulus and tangent modulus of the respective textile semi-finished products standardized to a fibre volume content of  $\varphi_f = 50\%$  according to German standard DIN EN ISO 2747 [14].

### *Experimentally determined strengths and corresponding failure modes*

Further based on the experimentally obtained results in the tensile tests the strength  $\sigma_{z,B}$  has been calculated. Fig. 7 shows the calculated tensile strengths  $\sigma_{z,B}$  according to the weighted average according to STELLBRINK [27] and the values indicated in the technical data sheets [18], both standardized to a fibre volume content  $\varphi_f = 50\%$ .

The tensile strengths  $\sigma_{z,B}$  determined experimentally and the values taken from the data sheets [18] indicated in Fig. 7 show different tendencies regarding the respective type of fabric reinforcement. The experimentally determined tensile strengths for the twill weave 2/2 reinforcement are partially significantly higher as the ones calculated by the indicated values in the data sheets. For the twill weave 1/3 the experimentally determined values and the indicated values in the data sheets [18] agree in a significantly higher degree. In fill direction the calculated values based on the indicated values in the technical data sheet [18] even result in such high values that cannot be achieved in the experiment. In weft direction the experimentally determined values correspond quite well, yet the standard deviation of the experimentally determined values has to be taken into account.

For completing the investigations and in order to properly interpret the results of the experimental tensile tests a careful analysis of the failure modes and crack propagation is carried out. Therefore pictures taken by a normal digital camera are used as well as pictures taken by optical microscopy. As the specimens with the same type of fabric reinforcement show analogous failure modes the corresponding pictures are displayed in Fig. 10 for the twill weave 2/2 and Fig. 11 for the twill weave 1/3, respectively.

Fig. 10 exemplarily shows pictures of a fractured specimen with fabric reinforcement of the type twill weave 2/2. Warp and fill direction ( $0^\circ$  and  $90^\circ$ ) show analogous failure modes. The crack starts in between the tabs near the centre at one side edge and proceeds perpendicularly to the applied load. Fig. 11 exemplarily shows pictures of a fractured specimens with fabric reinforcement of the type twill weave 1/3: Warp and fill direction ( $0^\circ$  and  $90^\circ$ ) once again show the same failure mode. In this case the crack starts in between the tabs near the centre at one side edge, too. In contrast the crack proceeds across the specimens in an angle of approx.  $45^\circ$  to the axis of the applied load. Details A, B and C in Fig. 11 show selected areas along the crack propagation taken under the optical microscope.



Figure 10: Exemplarily pictures of a fractured specimen with fabric reinforcement of the type twill weave 2/2 in warp direction ( $0^\circ$ ). Upper and lower left: Picture taken by a normal digital camera. Right: Picture taken under the optical microscope.

## CONCLUSIONS

**B**asalt fibre reinforced plastics with different fabric reinforcements are characterized mechanically. The carried out investigations contain experimental tensile tests and FE-analyses with representative volume elements (RVEs). The carried out investigations by FE-analyses with two types of RVEs are so validated experimentally. They allow quite accurate predictions of the stiffness in the predominant directions of a fabric reinforced plastics. Additionally the experimentally determined tensile strengths and corresponding failure modes are investigated. Finally the limits an outlook for the carried out FE-analyses based on RVEs are briefly mentioned.

The experimental determination of the fibre volume content, optical microscopy and the results from the tensile tests are the basis for the build-up of the RVEs and provide the input values for the numerical investigations. A high degree of



accordance shows the potentials in prediction of stiffnesses for fabric reinforced plastics by FE-analyses with RVEs. Yet, the presumptions made in the FE-model are simplifying, in parts even strongly. In spite of the presumptions regarding geometry and distribution of the fibre volume content the FE-analyses lead to results in the afore mentioned quality.

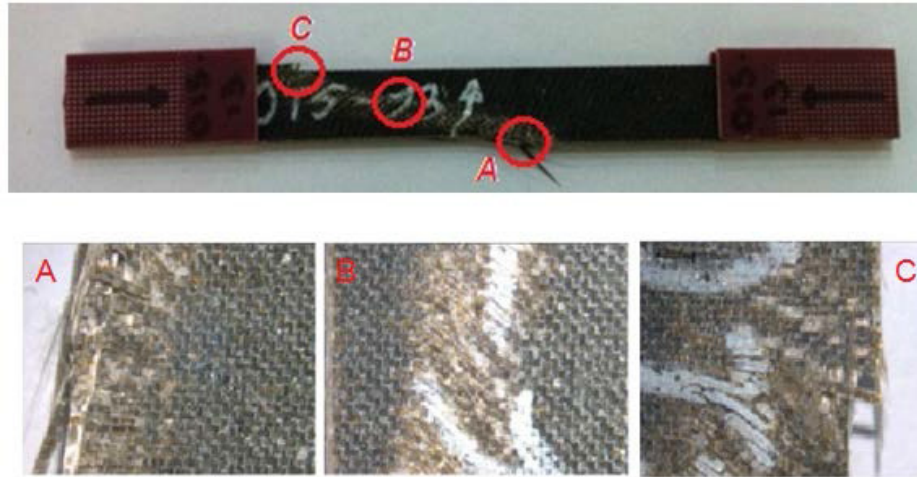


Figure 11: Exemplarily pictures of a fractured specimen with fabric reinforcement of the type twill weave 1/3 in fill direction ( $90^\circ$ ). Top: Picture taken by a normal digital camera. Bottom left to right: Pictures taken under the optical microscope along the crack propagation.

Whereas the determined stiffnesses are not affected by the type of yarn used in the fabric, the failure modes and the propagation of cracks are significantly affected through this parameter. Thus the geometry due to the construction of the fabric is sufficient for the determination of stiffnesses but not at all for failure modes and crack propagation. In fact the relative differences of the numerical determined stiffnesses compared to the mean values of the experimental ones are smaller than 1 %.

Thus the FE-analyses based on RVEs can be regarded as adequate to predict stiffnesses of fabric reinforced plastics with different geometries in the mesoscopic scale or even different kind of fibre reinforcement. Similar problems can be solved analogous, delivering reliable solutions already in a first approximation. The thereby obtained results then allow an extension through repeated alignment to the dimension of the real specimens or to the geometry of structural parts in application. So the determination of the stiffness of a structure in the linear-elastic range is permitted.

Even the influence of the fibre volume content on the stiffnesses is considered in the FE-calculations by investigating the experimentally determined as well as the standardized value. So even varying this very important parameter the determination of the stiffnesses is possible in a small but practically extremely relevant range.

The carried out FE-analyses do not include the determination of strengths and corresponding failure mode. Yet they the strengths are determined experimentally and the failure modes are described in detail. The afore mentioned properties are relevant topics to implement in further investigations.

## ACKNOWLEDGEMENTS

INCOTELOGY LTD. is acknowledged for providing the fabrics of basalt fibres. Further thanks go to Mr M. Eisenried (Laboratory for Composite Technology (LFT - Labor für Faserverbundtechnik) at the Department of Mechanical Engineering at the University of Applied Sciences Regensburg) for proofreading and for generating the schematic illustrations in the CAD-System.

## REFERENCES

- [1] E. J. Barbero, R. Luciano, *International Journal of Solid Structures*, 32, (1995) 1859.
- [2] C. C. Chamis, *SAMPE Quarterly*, (1984) 14.
- [3] T. Deák, T. Czigány, *Textile Research Journal*, 79 (7) (2009) 645



- [4] L. Fahrmeir, R. Künstler, I. Pigeot, G. Tutz, *Statistik – Der Weg zur Datenanalyse*. 5. Auflage, Springer-Verlag, Berlin/Heidelberg, (2005).
- [5] B. Jungbauer, M. Romano, I. Ehrlich, *Bachelorthesis, University of Applied Sciences Regensburg, Laboratory of Composite Technology, Regensburg*, (2012).
- [6] E. Lauterborn, *Dokumentation Ultraschalluntersuchung Eingangsprüfung, Internal Report wiweb Erding, Erding*, October (2011).
- [7] V. Lopresto, C. Leone, I. De Iorio, *Composites: Part B*, 42 (4) (2011) 717.
- [8] R. Luciano, E. Sacco, *European Journal of Mechanics – A/Solids*, 17(4) (1998) 599.
- [9] E. Mazzeo, G. Tenuta, F. Furgiuele, *Determinazione di proprietà meccaniche delle fibre di basalto in matrice polimerica termoindurente in maniera distruttiva (usando materiali laminati e prepreg)*. Tesi di specializzazione, Università della Calabria, Dipartimento di Meccanica, Cosenza, (2012).
- [10] K. Moser, *Faser-Kunststoff-Verbund – Entwurfs- und Berechnungsgrundlagen*. VDI-Verlag, Düsseldorf, (1992).
- [11] N. K. Naik, *Woven Fabric Composites*. Technomic Publishing Co., Lancaster (PA), (1994).
- [12] Bericht 2004-1535 – Prüfung eines Sitzes nach BS 5852:1990 section 5 – igniton source crib 7, für die Fa. Franz Kiel GmbH&Co. KG. Siemens AG, A&D SP, Frankfurt am Main, (2004).
- [13] DIN EN 2559 – Luft- und Raumfahrt – Kohlenstoffaser-Prepregs – Bestimmung des Harz- und Fasermasseanteils und der flächenbezogenen Fasermasse. Normenstelle Luftfahrt (NL) im DIN Deutsches Institut für Normung e.V., Beuth Verlag, Berlin, (1997).
- [14] DIN EN 2747 – Luft- und Raumfahrt – Glasfaserverstärkte Kunststoffe – Zugversuch. Normenstelle Luftfahrt (NL) im DIN Deutsches Institut für Normung e.V., Beuth Verlag, Berlin, (1998).
- [15] DIN EN ISO 1172 – Textilglasverstärkte Kunststoffe – Prepregs, Formmassen und Lamine – Bestimmung des Textilglas- und Mineralfüllstoffgehalts – Kalzinierungsverfahren. Normenausschuss Kunststoffe (FNK) im DIN Deutsches Institut für Normung e.V., Normenstelle Luftfahrt (NL) im DIN, Beuth-Verlag, Berlin, (1998).
- [16] DIN V 65352 – Luft- und Raumfahrt – Verfahren zur statistischen Auswertung der Prüfergebnisse bei der Qualifikations- und Abnahmeprüfung von Faserverbundwerkstoffen. Normenstelle Luftfahrt (NL) im DIN Deutsches Institut für Normung e.V., Beuth-Verlag, Berlin, (1987).
- [17] Epoxidharz L, Härter L – Technische Daten. Technical Data Sheet by R&G, (2011).
- [18] Quality Certificates for Fabrics and Rovings. Incotology Ltd., Bonn, January (2012).
- [19] J. Nolf, *Basalt fibres fire blocking textiles*, TUT, 49 (2003) 39.
- [20] P. Ottawa, M. Romano, M. Wagner, I. Ehrlich, N. Gebbeken, In: *Proceedings of the 11. LS-DYNA Forum, Ulm*, (2012).
- [21] B. Ozgen, H. Gong, *Textile Research Journal*, 81 (2010) 738.
- [22] L. Papula, *Mathematische Formelsammlung für Naturwissenschaftler und Ingenieure*. 10. Auflage, Vieweg+Teubner, Wiesbaden, (2009).
- [23] D. Saravanan, *IE(I) Journal-TX*, 86 (2006) 39.
- [24] V. Schmid, B. Jungbauer, M. Romano, I. Ehrlich, N. Gebbeken, In: *Proceedings of the Applied Research Conference, Regensburg*, (2012).
- [25] V. Schmid, B. Jungbauer, M. Romano, I. Ehrlich, N. Gebbeken, In: *Proceeding of the Applied Research Conference, Regensburg*, (2012).
- [26] H. Schürmann, *Konstruieren mit Faser-Kunststoff-Verbunden*. Springer-Verlag, Berlin/Heidelberg/New York, (2005).
- [27] K. Stellbrink, *Micromechanics of Composites*. Hanser-Verlag, München/Wien, (1996).
- [28] T. Wittek, T. Tanimoto, *express Polymer Letters*, 2 (11) (2008) 810, [www.expresspolymlett.com](http://www.expresspolymlett.com), DOI: 10.3144/expresspolymlett.2008.94